Kinetic Features of the Radical Species Produced in γ-Irradiated dl-Tartaric Acid and the Dosimetric Potential of this Acid

H. Tuner[a,1] and M. Korkmaz[b]

[a] Department of Physics, Faculty of Science, Balikesir University, Çağış, 10145, Balikesir, Turkey; and [b] Department of Physics
Engineering, Faculty of Engineering, Hacettepe University, Beytepe Ankara, Turkey

Tuner, H. and Korkmaz, M. Kinetic Features of the Radical Species Produced in γ-Irradiated dl-Tartaric Acid and the Dosimetric Potential of this Acid. *Radiat. Res.* **172**, 120–128 (2009).

The room-temperature and high-temperature kinetic features of the radical species produced in solid dl-tartaric acid (dl-TA) γ-irradiated at room temperature and the dosimetric potential of this acid were investigated in a detailed ESR study. Irradiated dl-TA presents an ESR spectrum with many unresolved resonance lines even at the lowest radiation dose applied (100 Gy). The evolution of the signal intensities associated with induced radical species with microwave power, applied dose and temperature was followed. Three groups of resonance intensities originating from three different radicals exhibiting different spectroscopic features, stabilities at room and high temperatures, and radiation yields were found to take part in the formation of experimental ESR spectrum. These three species were calculated to exhibit spectroscopic features similar to those already reported for X- or γ-irradiated deuterated single crystals of dl-TA and assigned as I, II and III. The same radical notation was adopted in the present work, and the intensities related to these species were denoted with the names of their corresponding species. Species III, which had the lowest radiation yield and the lowest stability, was observed as a species of four resonance lines. The two inner constituents of these four lines were partially obscured by the two central doublets originating from species I and II. The latter were relatively stable and had activation energies around 35 kJ/mol. The percentage concentrations of the involved species were estimated by comparing experimental and calculated spectra. The reasonably high radical yields of the dl-TA in the dose range of interest, the fairly good stabilities of the species produced (I and II) at room temperature, and the almost linear features of the constructed dose–response curves led us to conclude that the intensities associated with the stable species (I and II) could be used to estimate the applied dose in the dose range of 100 Gy–34 kGy with fairly good accuracy and that dl-TA could be a good candidate for exploring low radiation dose measurements by ESR dosimetry. © 2009 by Radiation Research Society

[1] Address for correspondence: Department of Physics, Faculty of Science, Balikesir University, Çağış, 10145, Balikesir, Turkey; e-mail: htuner@hacettepe.edu.tr.
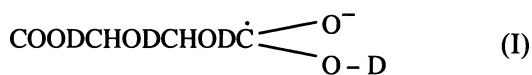
INTRODUCTION

Several years ago electron spin resonance (ESR) spectroscopy was proposed as a method for measurement of radiation dose. L-Alanine is the material of choice as a dosimeter due to its characteristic features such as reasonable radiation sensitivity, a very stable free radical signal, an excellent tissue equivalence, and a linear dose–response curve. Although work carried out by different research groups on alanine was promising for the measurement of low radiation doses (1–4), it would be interesting to explore new materials that are sensitive to low doses if ESR is to become a serious alternative to existing methods of dose measurement. The following criteria must be met by such materials: a high radical yield, a linear dose–response curve, sharp spectral lines, and a stable signal at room temperature (5, 6). Ammonium tartrate, 2-methylalanine, compounds of formic acid and dithionate salts have been evaluated (5–12).

The spectroscopic features of the radical species produced in deuterated dl-tartaric acid (dl-TA) single crystals γ- and X-irradiated at room temperature, 77 K and 195 K were investigated in three previous studies (13–15). Rao and Gordy (13) reported that the principal radical observed when deuterated dl-TA is γ-irradiated at room temperature is

$$\text{COOD}\overset{\cdot}{\text{C}}\text{ODCHODCOOD} \qquad (\text{II})$$

The spectrum of this radical at room temperature was proposed to be a slightly anisotropic doublet near $g = 2.0036$ with a maximum hyperfine splitting of 0.65 mT. The same radical (II) has also been observed in a dl-TA crystal X-irradiated at 77 K when it was allowed to warm to room temperature (14). In another study of deuterated dl-tartaric acid monohydrate single crystal X-irradiated at 77 K, Moulton and Cernansky (15) reported the presence of an ionic radical (I) giving rise to a doublet with a relatively high hyperfine splitting.

In a later study of the same compound X-irradiated at 195 K, the same authors reported the existence of Radical III in addition to Radical I (15).

120

$$COODCHODCHOD\overset{\centerdot}{C}\underset{O-D}{\overset{O^-}{\diagup\diagdown}} \qquad (I)$$

$$^{\centerdot}CHODCHODCOOD \qquad (III)$$

Radical III presents a four-line spectrum representing hyperfine coupling to two hydrogen atoms, one an α hydrogen and the other a β hydrogen. When the temperature was increased to room temperature, Radical III was observed to decay to Radical II (13, 15).

Although the low- and room-temperature spectroscopic features of the radicals produced in X- or γ-irradiated dl-tartaric acid were investigated in detail in the previous studies, to our knowledge, no attempt has been made to determine its dosimetric potential. Therefore, the aim of this exploratory work was to investigate the dosimetric potential of dl-TA in low (100–1000 Gy) and intermediate (1–34 kGy) dose ranges through an elaborate ESR study of the room- and high-temperature kinetic features of the radical species produced upon γ irradiation of this compound at room temperature.

MATERIALS AND METHODS

Spectroscopic-grade dl-TA was provided by GMT Food Ingredients Company (Istanbul) and was stored at room temperature in a well-sealed container protected from light and humidity changes. No further purification was performed. Samples with particle sizes smaller than 1 μm were used throughout the experiment to avoid effects of orientation on recorded spectra. dl-TA is a colorless or translucent crystalline powder with no odor. The melting point is about 200–206°C with decomposition when it is heated rapidly in a sealed capillary tube. Its molecular structure is shown in Fig. 1. It is made of low-atomic-number elements, like soft tissue. All irradiations were performed at room temperature using a ^{60}Co GammaCell at a dose rate of 1.41 kGy/h at the Sarayköy Establishment of Turkish Atomic Energy Agency in Ankara. The dose rate at the sample sites was measured by a Fricke dosimeter with an uncertainty of ±1 Gy/min within a confidence level of 85%. Investigations were performed on samples irradiated at 13 different doses (100, 250, 500, 750, 1 × 10^3, 2 × 10^3, 3 × 10^3, 5 × 10^3, 7 × 10^3, 1.0 × 10^4, 1.5 × 10^4, 2.5 × 10^4 and 3.4 × 10^4 Gy).

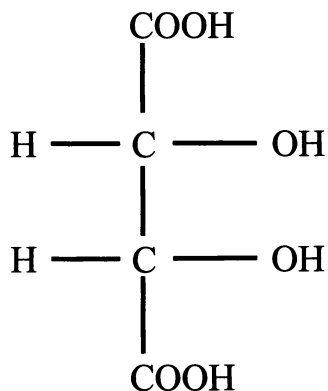ESR measurements were carried out on samples in standard ESR tubes using a Bruker EMX 131 X-band spectrometer operating at 9.8 GHz and equipped with a high-sensitivity cylindrical cavity. Signal intensities were calculated both from first-derivative spectra directly and from double integration of the recorded first-derivative spectra and compared with that obtained for a standard sample (DPPH) under the same spectrometer operating conditions. The sample temperature inside the microwave cavity was monitored with a digital temperature control system (Bruker ER4131-VT) that measured the temperature with an accuracy of ±0.5 K at the site of sample. A cooling, heating and subsequent cooling cycle was adopted to monitor the evolutions of the ESR line shape with temperature using samples irradiated at room temperature. Variations in the spectrum pattern and in the resonance line intensities with microwave power at room temperature and at 130 K were also studied in the range of 0.005–2.5 and 0.001–1.0 mW, respectively.

The kinetic behaviors of the contributing radical species were determined at different temperatures through annealing studies performed at 370, 380, 390 and 400 K. The samples irradiated at room temperature were heated inside the microwave cavity to predetermined temperatures and kept at these temperatures for a predetermined time; then their ESR spectra were recorded. The results were the averages of five replicates for each radiation dose.

RESULTS

General Features of the ESR Spectra; Variation with Applied Dose and Microwave Power

Although unirradiated dl-TA exhibited no ESR signal, samples irradiated at room temperature showed ESR spectra consisting of many unresolved resonance lines, making them more complex than the spectrum obtained for deuterated dl-TA (13–15). The room-temperature spectra recorded for three samples irradiated at three different radiation doses are given in Fig. 2a, b and c. An evaluation technique based on monitoring the evolutions under different experimental conditions of the intensities associated with three contributing species (I, II and III) named in accordance with the previous ESR results on X- and γ-irradiated dl-

$$\begin{array}{c} COOH \\ | \\ H \text{——} C \text{——} OH \\ | \\ H \text{——} C \text{——} OH \\ | \\ COOH \end{array}$$
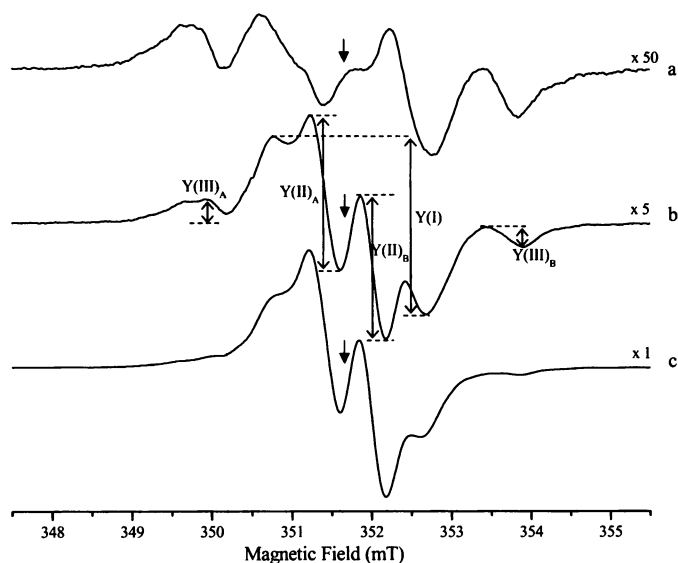
FIG. 1. Molecular structure of dl-TA.

FIG. 2. Room-temperature ESR spectra of dl-TA irradiated with (a) 100 Gy, (b) 5 kGy and (c) 34 kGy. Arrows indicate the position of DPPH resonance line ($g = 2.0036$).

TA (*13–15*) was adopted throughout the study. Inspection of the spectra shown in Fig. 2a, b and c indicates that all intensities increase with the increase in the applied radiation dose but with different rates of increase and that the general spectral pattern is conserved over the entire dose range used (100 Gy–34 kGy) with the exception of the appearance of a new narrow doublet at the center of the spectrum that is attributable to a radical species of type II reported by Rao and Gordy (*13*). Although the intensities $Y(II)_A$ and $Y(II)_B$, which describe the central narrow doublet, are hardly discernible at 100 Gy, they are clearly developed at 500 Gy, and above 500 Gy they become the dominant features of the experimental spectrum above about 5 kGy. This shows that radical species of different radiation yields are being produced in γ-irradiated dl-TA as in the case of deuterated single crystal of dl-TA (*13–15*). The narrow central doublet specified by the $Y(II)_A$ and $Y(II)_B$ intensities has a *g* value of 2.0038 and a hyperfine splitting of about 0.7 mT. The separation between relatively weak unstable lines appearing at the lowest and highest magnetic fields and having intensities of $Y(III)_A$ and $Y(III)_B$ (Fig. 2b and c) is about 4.4 mT. These lines are believed to constitute the two side resonance lines of a four-line ESR signal originating from species III. This result implies the existence of radical species exhibiting large hyperfine splitting in dl-TA γ-irradiated at room temperature. A four-line species of even greater hyperfine splitting, called radical III, has also been identified by Moulton and Cernansky (*15*) in dl-TA X-irradiated at 195 K. This four-lines species was reported to exhibit a spread of about 7 mT in the experimental spectrum of the dl-TA single crystal (*15*). A smaller spread less than about 6 mT was observed in the present work. This is merely due to the fact that powder samples generally have smaller spectral extents single-crystal spectra. The stable lines contributing to both sides of the central narrow doublet originating from species II were thought to be the two constituents of another doublet screened by the central lines of species II and III. The ionic radical denoted as I was believed to be responsible from these hyperfine lines of hyperfine splitting about 2.0 mT as in the case for X- or γ-irradiated deuterated dl-TA (*13–15*). The evolution under different experimental conditions of the latter species was monitored by measuring the intensity of Y(I) (Fig. 2b).

Intensities normalized to the receiver gain, the mass of the sample, and the intensity of the standard were used in the calculations. Variations in the intensities of the various spectral components with applied microwave power were studied both at room temperature (290 K) and at 130 K. The results associated with intense and stable Y(I), $Y(II)_A$ and $Y(II)_B$ intensities (*13–15*) are presented in Fig. 3a and b. At room temperature and 130 K, the measured intensities saturate homogeneously with different rates

due to the presence of radicals of more than one kind exhibiting different saturation characteristics in γ-irradiated dl-TA as in the case of X- or γ-irradiated deuterated dl-TA (*13–15*). In the microwave power range investigated, the weak unstable $Y(III)_A$ and $Y(III)_B$ intensities the appear at both sides of the experimental spectrum were observed to exhibit the characteristic feature of inhomogeneously broadened resonance lines at room temperature (290 K) and at 130 K.

The percentage concentration weights of species I, II and III for the experimental spectra were also calculated by a spectrum simulation technique. The intensity data derived from two spectra recorded just after irradiation for two samples irradiated with doses of 100 Gy and 10 kGy were used for this purpose, and the following values were obtained: 100 Gy [I (0.26); II (0.03); III (0.71)] and 10 kGy [I (0.26); II (0.69); III (0.05)].
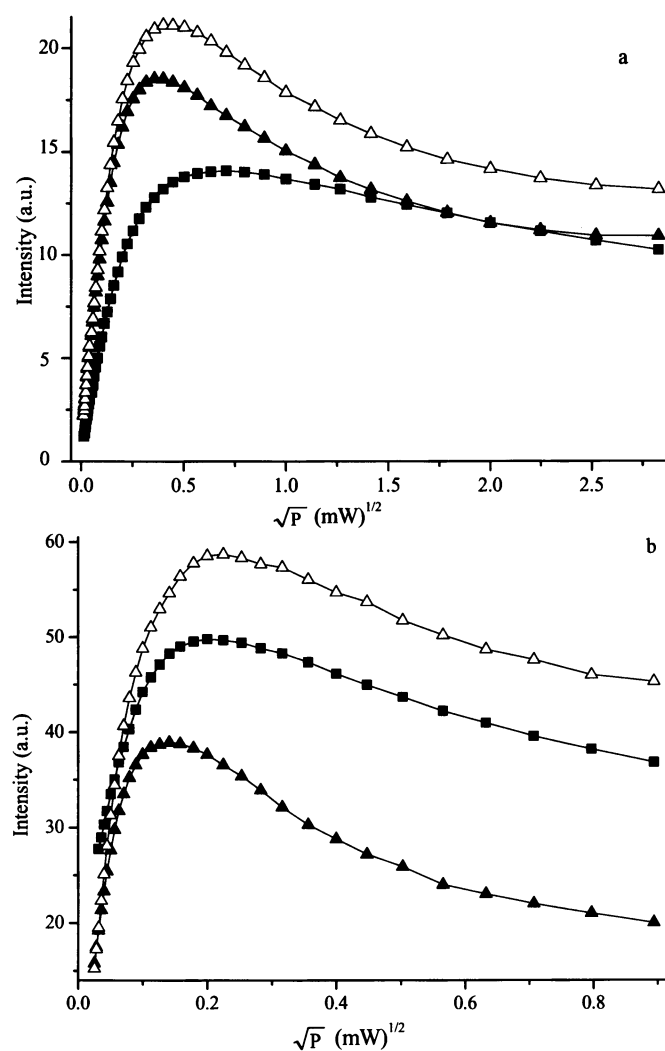

FIG. 3. Variations of the intensities of stable intense resonance lines with applied microwave power at two different temperatures for a sample irradiated with a dose of 10 kGy at (panel a) room temperature (290 K) and (panel b) 130 K. Y(I) (■); $Y(II)_A$ (▲); $Y(II)_B$ (△).

Kinetic Features of the Radical Species

The effects of temperature, storing time and annealing at high temperatures on the spectrum pattern and on the assigned intensities (Fig. 2b) were investigated. A cooling, heating and cooling cycle was adopted to monitor the evolution of the spectrum with temperature using samples irradiated with a dose of 10 kGy at room temperature. Spectra were recorded at low microwave powers to avoid any microwave power saturation at low temperatures. The sample temperature first decreased to 130 K from room temperature (290 K), then increased to 400 K at increments of 20 K, and finally decreased again to room temperature with the same decrements. No pattern changes were observed in the temperature range studied except the expected decreases and increases in the intensities. The variations with temperature of the intensities of some intense stable lines and the spectrum areas calculated by the double integration technique are given in Fig. 4. The intensities and spectrum areas experience reversible changes over a wide temperature range, but these changes have irreversible characteristics after reacting temperatures above 290 K due to the decay of the radical species involved by radical-radical recombination reactions at high temperatures. The reversible increases of different magnitudes observed in the intensities below room temperature likely originate from the presence of the radical species that have different microwave saturation characteristics at low temperatures. Namely, below room temperature, variation in the intensity of a given resonance line is determined to a large extent by the microwave saturation characteristics of the most significantly contributing radical or radicals. This variation can be a decrease or an increase depending on whether it (they) was (were) saturated or not at low temperatures.
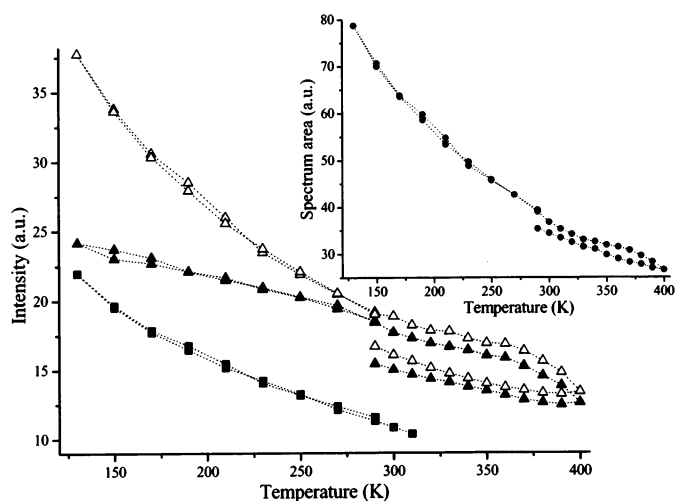
The room-temperature stabilities of the radical species produced after irradiation are important from the point of view of the dosimetric properties of the investigated compounds. Therefore, long-term variations in the intensities of assigned resonance lines were also studied. The assigned resonance intensities do not show the same dependence on the applied radiation dose. As is emphasized in the previous section, intensities $Y(II)_A$ and $Y(II)_B$ are hardly distinguishable below 500 Gy, but they heavily dominate the experimental spectrum at high dose, making reliable determination of $Y(I)$, $Y(III)_A$ and $Y(III)_B$ intensities difficult. Thus samples irradiated with different doses were used to achieve this goal. The variations with storage time in the assigned intensities of the samples irradiated at low (100 Gy) and high (10 kGy) doses and stored in a well-sealed container at room temperature (290 K) were used to study the decay of the radical species responsible from unstable weak $[Y(III)_A; Y(III)_B]$ and intense stable $[Y(I); Y(II)_A; Y(II)_B]$ line intensities, respectively. Data collected from samples irradiated at low dose (100 Gy) indicated that the decrease in the $Y(III)_A$ and $Y(III)_B$ weak intensities caused an increase in the intensity of the central narrow doublet ($Y(II)_A$ and $Y(II)_B$) appearing just at the center of the experimental spectrum (Fig. 2b). In other words, the radical species responsible from weak $Y(III)_A$ and $Y(III)_B$ intensities decay to species giving rise to the narrow central doublet having $Y(II)_A$ and $Y(II)_B$ intensities during storage at room temperature. Two spectra recorded just after and 24 h after irradiation are given in Fig. 5. It is seen that although the $Y(I)$ intensity is almost conserved over the storage period of 24 h, the $Y(III)_A$ and $Y(III)_B$ weak intensities are almost completely lost and the central narrow doublet intensifies proportionally over the same period. Room-temperature

FIG. 4. Variations of the intensities of some characteristic resonance lines and spectrum area with temperature. $Y(I)$ (■); $Y(II)_A$ (▲); $Y(II)_B$ (△). Inset: spectrum area (●) calculated by double integration.
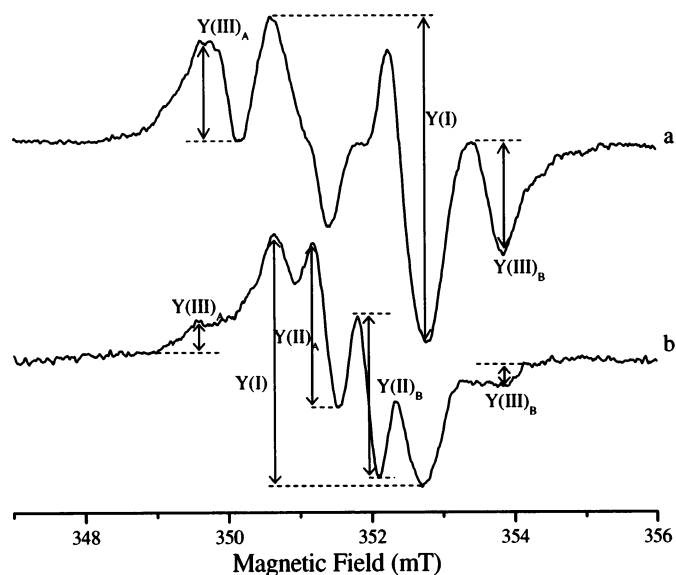

FIG. 5. ESR spectra of a sample irradiated with a dose of 250 Gy (panel a) just after and (panel b) 24 h after irradiation.

decay data relevant to Y(III)$_A$ and Y(III)$_B$ weak intensities derived for a sample irradiated with 100 Gy are presented in Fig. 6. The decay characteristics of the radical species responsible from the Y(I), Y(II)$_A$ and Y(II)$_A$ intense resonance lines were also investigated using a sample irradiated at relatively high dose (10 kGy). The variations with the storage time of the intensities of intense resonance lines are presented in Fig. 7 for a storage period of 85 days. From the data in this figure, it is obvious that the radical species responsible for the experimental spectrum of γ-irradiated dl-TA are not stable at room temperature under normal conditions. Principal intense lines labeled as Y(I), Y(II)$_A$ and Y(II)$_B$ were observed to exhibit similar decay behaviors over the entire storage period (85 days). The percentage decreases in the intensities of these resonance lines were calculated to be about 5.0, 9.0 and 6.0, respectively, at the end of a storage period of 10 days.

The decays of the radical species in annealed samples were also studied to determine the kinetic features of the species responsible from experimental ESR spectra at high temperatures. The decay rates of radical species depend on the nature of the matrix containing these species, and annealing is a constant process, with local diffusion of radicals and molecules in the matrix (*16*). Annealing studies were performed at four different temperatures (370 K, 380 K, 390 K and 400 K) over a period of 60 min. Samples irradiated with a dose of 10 kGy and stored at room temperature for 3 days were used to minimize or even to cancel out the contribution of the short-lived species giving rise to four weak lines whose two easily distinguishable components are Y(III)$_A$ and Y(III)$_B$. The results obtained for Y(I) and Y(II)$_B$ intensities at four different annealing temperatures are given in Fig. 8 as an example of these variations.
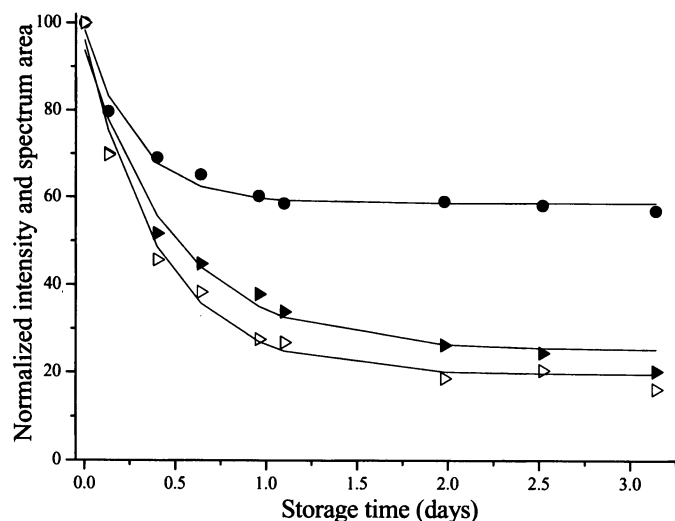

FIG. 6. Variations of the weak intensities lines and spectrum area with time under normal storage conditions (290 K and open to atmosphere). Y(III)$_A$ (▶); Y(III)$_B$ (▷); spectrum area (●).
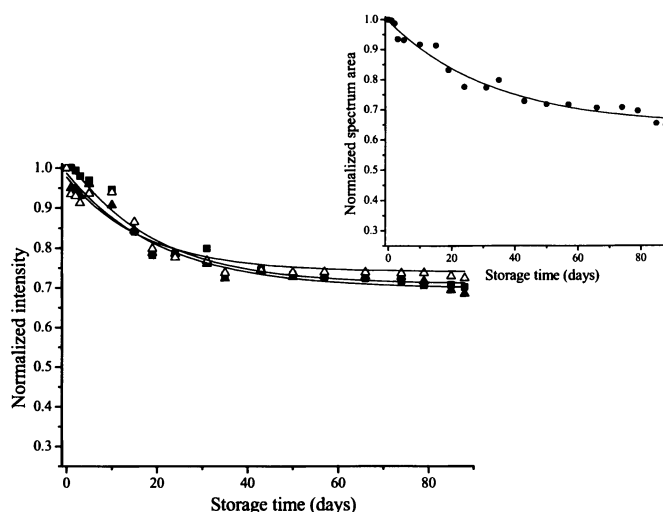

FIG. 7. Variations of the intensities of intense resonance lines with storage time under normal storage conditions. Y(I) (■); Y(II)$_A$ (▲); Y(II)$_B$ (△) and spectrum area (●).

Intensity decay data were fitted by a mathematical function consisting of the sum of two exponential functions decaying differently based on the information drawn from spectra recorded just after and 24 h after irradiation (Fig. 5), namely, assuming that the doublets taking part at the center of the spectrum were associated with two radical species with different decay characteristics. Decay constants calculated by this technique were used to derive the activation energies of the radical species contributing to the formation of the intense and relatively stable central doublets. Species of types I and II having the structures specified in the Introduction and activation energies of 32.7 ± 1.7 kJ/mol and 38.5 ± 2.1 kJ/mol are believed to be the species responsible for the two central doublets, one with larger and one with smaller (narrow one) hyperfine splitting, respectively. It is seen that the activation energies of species I and II produced in γ-irradiated dl-TA are relatively low and that they decay relatively fast at high temperatures.

Dosimetric Features of dl-TA

A higher concentration of radicals generated at the same absorbed dose of radiation indicates a higher sensitivity of the substance to the type of the radiation used. Therefore, the radiation sensitivity and consequently the dosimetric potential of dl-TA were also studied through the variation of the Y(I), Y(III)$_A$ and Y(III)$_B$ intensities at low (100 Gy–000 Gy) and Y(I) and Y(II)$_A$ and Y(II)$_B$ at intermediate (1 kGy–34 kGy) doses (Fig. 2b). The results are presented as dose–response curves in the low- (100 Gy–1000 Gy) and intermediate-dose (1 kGy–34 kGy) regions (Fig. 9 and Fig. 10). The choice of appropriate functions to fit experimental data is an important step in the development of radiation dosimetry. The mathematical functions given in Table 1
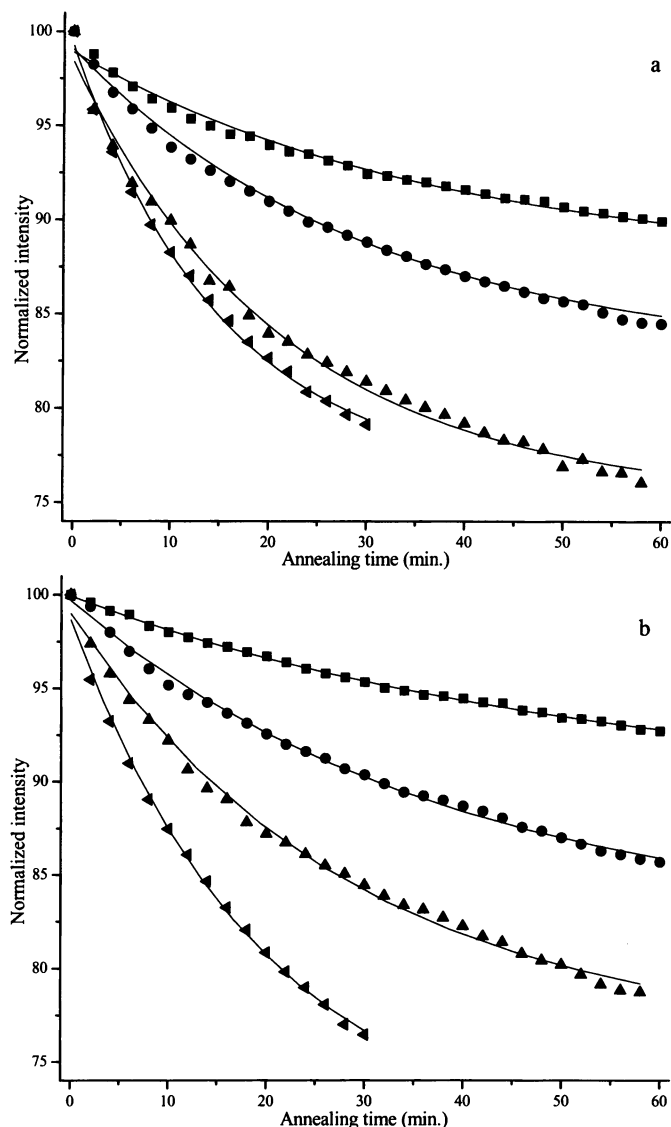
FIG. 8. Variations of line intensities at four different annealing temperatures. Panel a: Y(I); panel b: Y(II)$_B$. 370 K ($\blacksquare$); 380 K ($\bullet$); 390 K ($\blacktriangle$); 400 K ($\blacktriangleleft$).

were used to describe the variations of the specified intensities (Fig. 2b) and spectrum area under the absorption curve. In these functions, Y and D represent the ESR signal intensity and absorbed dose in kGy, respectively, and a, b, c... etc. are the constants to be determined. No attempt has been made to force the regression curves to pass through the origin. The limits of detection and quantification predicted by S/N = 3 and the S/N = 10, respectively, have been determined to be 100 Gy and 500 Gy after ten successive accumulations of ESR spectra. From a comparison of regression coefficients given in Table 1, it is seen that a linear function of absorbed dose including a quadratic term describes best the spectrum area data (Y$_1$) calculated by two successive integrations of the experimental first-derivative spectra and measured signal intensity data such as Y(III)$_A$, Y(I) and Y(II)$_A$ in the low- (100–1000 Gy) and intermediate- (1 kGy–34 kGy) dose regions.
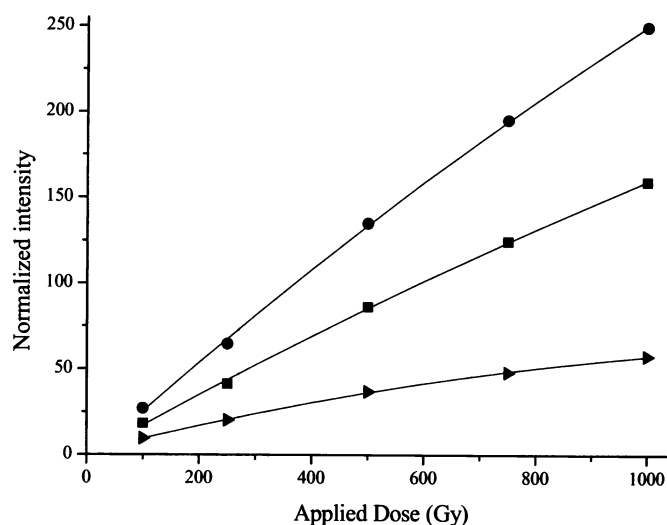

FIG. 9. Dose–response curves obtained in the range of 100–1000 Gy. Symbols: experimental data points; lines: calculated using Y = c + d D + q D^2 function. Y(III)$_A$ ($\blacktriangleright$); Y(I) ($\blacksquare$); spectrum area ($\bullet$).

The usefulness of the proposed method and mathematical functions in the estimation of applied doses was tested by a back-calculation technique. Briefly, this is done by entering the measured ESR signal intensities in the proposed mathematical functions and calculating the doses. The results are expressed as graphs of calculated and applied doses. The graphs constructed using a quadratic function and experimental Y(I) signal intensity data were found to give best slopes, intercepts and regression coefficients in the low- and intermediate-dose regions and are presented in Fig. 11. The other graphs are not shown.

The following conclusions were drawn from dosimetric studies performed on dl-TA. The shapes of the dosimetric curves constructed using peak-to-peak signal intensities are linear in both dose regions (100–1000 Gy
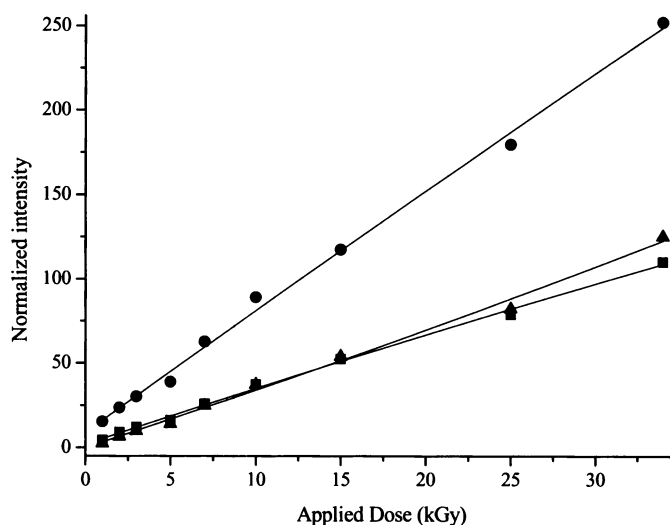

FIG. 10. Dose–response curves obtained in the range of 1–34 kGy. Symbols: experimental data points; lines calculated using function I = c + d D + q D^2, Y(I) ($\blacksquare$); Y(II)$_A$ ($\blacktriangle$); spectrum area ($\bullet$).

TABLE 1
Mathematical Functions Used to Describe Experimental Dose–Response Data Derived in Two Different Dose Regions and Calculated Coefficients

Function		Dose range					
		100 Gy–1000 Gy			1 kGy–34 kGy		
		Measured quantities			Measured quantities		
		Y_1*	Y(I)	$Y(III)_A$	Y_1*	Y(I)	$Y(II)_A$
Linear	a	4.27184	3.51533	6.65351	9.74483	2.79070	−1.28146
Y = a + bD	b	0.2504	0.15885	0.05354	7.07715	3.15624	3.61191
		$(0.99773)^\dagger$	$(0.99799)^\dagger$	$(0.98289)^\dagger$	$(0.99648)^\dagger$	$(0.99710)^\dagger$	$(0.99449)^\dagger$
Linear-quadratic	c	−3.95745	−1.05834	1.35759	8.75387	1.79196	−0.00296
$Y = c + dD + qD^2$	d	0.29729	0.18491	0.08372	7.31934	3.40033	3.29945
	q	−0.00004	−0.00002	−0.00003	−0.00719	−0.00725	0.00928
		$(0.99959)^\dagger$	$(0.99942)^\dagger$	$(0.99948)^\dagger$	$(0.99656)^\dagger$	$(0.99750)^\dagger$	$(0.99500)^\dagger$
Power	f	0.37703	0.25235	0.35344	10.83623	4.30856	3.11153
$Y = fD^g$	g	0.94211	0.93509	0.7402	0.88669	0.91575	1.04102
		$(0.99863)^\dagger$	$(0.99882)^\dagger$	$(0.99572)^\dagger$	$(0.99592)^\dagger$	$(0.99768)^\dagger$	$(0.99468)^\dagger$
Exponential	h	1145.34300	722.68680	86.075160	779.29053	418.96020	2513.93479
$Y = h(1 - e^{-jD})$	j	0.00025	0.00025	0.0011	0.0112	0.00882	0.00144
		$(0.99929)^\dagger$	$(0.99934)^\dagger$	$(0.99944)^\dagger$	$(0.99372)^\dagger$	$(0.99695)^\dagger$	$(0.99335)^\dagger$
Sum of two exponential	k	597.2351	364.88167	52.16253	3699.13748	4600.42326	2138.99668
$Y = k(1 - e^{-mD}) +$	m	0.00024	0.00025	0.00145	0.00197	0.00067	0.00084
$n(1 - e^{-pD})$	n	597.2351	357.80513	62.72794	9.0476	5.75812	2122.61384
	p	0.00024	0.00025	0.00033	2.13824	0.20313	0.00084
		$(0.99929)^\dagger$	$(0.99934)^\dagger$	$(0.99946)^\dagger$	$(0.99658)^\dagger$	$(0.99778)^\dagger$	$(0.99363)^\dagger$

* Y_1: Spectrum area; † correlation coefficients.

and 1–34 kGy), but the best results are obtained for Y(I) signal intensity associated with radical species I. The highest uncertainties on the applied doses determined by back-calculation technique were calculated to be 7% and 5% in the low- and intermediate-dose regions for Y(I) and $Y(II)_A$ intensities, respectively. Therefore, the use of linear regression may be technically feasible for radiation dose estimation in both regions if dl-TA is used as a

FIG. 11. Graph comparing back-calculated dose to applied dose graph constructed using Y_1 (spectrum area) data. Intermediate-dose (1–34 kGy) region (intercept: 0.0002; slope: 1.0000; r^2: 0.99659). Inset: low-dose (100–1000 Gy) region (intercept: 0.0500; slope: 0.98948 and r^2: 0.9996).

dosimetric material. This result turns out to be important in the measurement of low radiation doses by ESR spectroscopy.

DISCUSSION

From the evolution of the monitored signal intensities (Fig. 2b) with applied radiation dose, microwave power and temperature, it was concluded that these intensities could be divided into three subgroups related to different kinds of radical species already reported in the literature for deuterated dl-TA (13–15). $Y(III)_A$ with $Y(III)_B$ and Y(I) intensities are related to the radical species III and I, respectively, having the structures given in the Introduction. $Y(II)_A$ and $Y(II)_B$ intensities, which are related to another species, are hardly discernible below 500 Gy just after irradiation (Fig. 5), but they dominate the ESR spectrum above 5 kGy even just after irradiation (Fig. 2c). Radical II with the structure given in the Introduction was considered to be the species responsible for the $Y(II)_A$ and $Y(II)_B$ intensities, which form the two resonance lines of the central narrow doublet of hyperfine splitting about 0.7 mT. The unstable $Y(III)_A$ and $Y(III)_B$ intensities are the two components of a four-line ESR spectrum spread over a magnetic-field range larger than 4 mT originating from a radical produced by loss of a carboxyl group from the dl-TA molecule, that is, from radical species III. An unstable radical with an ESR spectrum
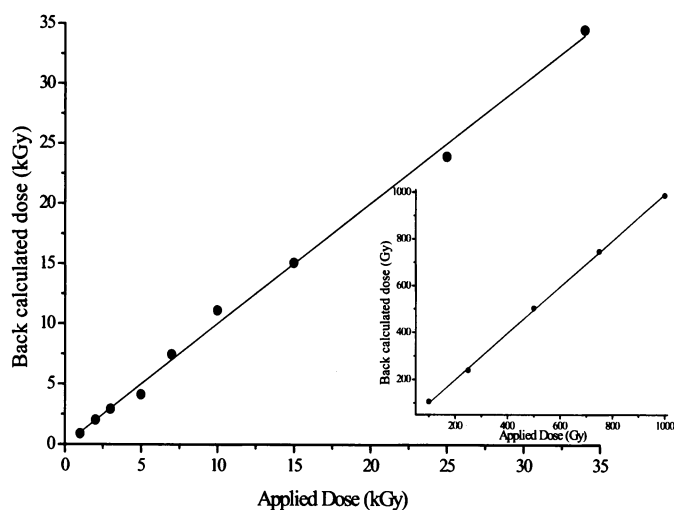
consisting of four resonance lines, which is similarly called Radical III, has also been reported in previous ESR studies carried out on deuterated dl-TA single crystals X- or γ-irradiated at low temperatures and observed at low temperatures (13, 15). Radical III has been reported (13, 15) to decay to another radical denoted as radical II exhibiting a hyperfine splitting about 0.7 mT. The decay of the monitored intensities of Y(III)$_A$ and Y(III)$_B$, which are predicted to constitute the lowest and the highest magnetic-field components of a quartet, to a narrow doublet of hyperfine splitting about 0.7 mT, was considered to be an indication of the similarity between the decay behaviors of the outermost spectrum components of X- or γ-irradiated deuterated single crystals of dl-TA and γ-irradiated protonated dl-TA. The radical causing a doublet of hyperfine splitting about 0.7 mT was supposed to be produced by breaking one of the C-H bonds on carbon backbone of dl-TA molecule, yielding to an intermediate exhibiting the structure of radical species II (13). The intensity of Y(I) is attributed to another radical species of different radiation yield and stability manifesting as a doublet of hyperfine splitting about 2 mT. This result was considered by observing the production of a radical species of type I in γ-irradiated dl-TA as in the case of irradiated deuterated dl-TA. Based on the above evaluations and in accordance with the previous ESR studies carried out on X- or γ-irradiated deuterated tartaric acid single crystals (13, 15), it was concluded that at least three radicals with different spectroscopic and kinetic features and different concentrations contribute to the formation of the observed experimental ESR spectrum of dl-TA γ-irradiated at room temperature. Radical III is the most unstable species and decays to species II a short time after irradiation. However, species I and II are more stable under laboratory conditions and have very similar activation energies (32.7 ± 1.7 kJ/mol and 38.5 ± 2.1 kJ/mol, respectively).

Dose–response curves associated with Y(I) and Y(II)$_A$ or Y(II)$_B$ intensities were used to estimate γ-radiation doses, and it was concluded that administered doses could be estimated with an accuracy of 7% and 5% in the dose regions 100–1000 Gy and 1–34 kGy, respectively, even a few days after irradiation.

CONCLUSION

Three radical species denoted as I, II and III were found to be produced in γ-irradiated dl-TA. They have spectroscopic and kinetic features similar to those reported for species produced in X- or γ-irradiated single crystals of deuterated dl-TA (13–15). At room temperature, III is the most unstable of the observed species, and it is transformed into II a short time after irradiation. Depending on the dose applied, species are produced with different yields, and I and

II were found to dominate the experimental spectrum in the 100–1000-Gy and 1–34-kGy dose range, respectively.

Fairly high radical yields of the γ-irradiated dl-TA and the stabilities of the species produced over relatively long times after irradiation encouraged us to explore the dosimetric potential of dl-TA in measuring γ-radiation doses. Thus the dose–response curves associated with the stable species I and II (Figs. 9 and 10) were constructed and administered doses were calculated by a back-projection technique (Fig. 11). It was concluded that γ-radiation doses could be estimated with an accuracy of 7% and 5% in the dose regions 100–1000 Gy and 1–34 kGy, respectively, if the constructed dose–response curves were used. Therefore, dl-TA could be useful in measuring γ-radiation doses as low as 100 Gy.

REFERENCES

1. V. Nagy, S. V. Sholom, V. V. Chumak and M. F. Desrosiers, Uncertainties in alanine dosimetry in the therapeutic dose range. Appl. Radiat. Isot. 56, 917–929 (2002).

2. P. H. G. Sharpe, K. Rajendran and J. P. Sephton, Progress towards an alanine/ESR therapy level reference dosimetry service at NPL. Appl. Radiat. Isot. 47, 1171–1175 (1996).

3. M. Anton, Uncertainties in alanine/ESR dosimetry at the Physikalisch-Technische Bundesanstalt. Phys. Med. Biol. 51, 5419–5440 (2006).

4. F. Castro, F. Ponte and L. Pereira, Development of physical and numerical techniques of alanine/EPR dosimetry in radiotherapy. Radiat. Prot. Dosimetry 122, 509–512 (2006).

5. M. Ikeya, G. M. Hassan, H. Sasaoka, Y. Kinoshita, S. Takaki and C. Yamanaka, Strategy for finding new materials for ESR dosimeters. Appl. Radiat. Isot. 52, 1209–1215 (2000).

6. A. Lund, S. Olsson, M. Bonora, E. Lund and H. Gustafsson, New materials for ESR dosimetry. Spectrochim. Acta A 58, 1301–1311 (2002).

7. T. A. Vestad, E. Malinen, A. Lund, E. O. Hole and E. Sagstuen, EPR dosimetric properties of formates. Appl. Radiat. Isot. 59, 181–188 (2003).

8. E. Lund, H. Gustafsson, M. D. Danilczuk, M. Sastry and A. Lund, Compounds of ^{6}Li and natural Li for EPR dosimetry in photon/neutron mixed radiation fields. Spectrochim. Acta A 60, 1319–1326 (2004).

9. S. E. Bogushevich and I. I. Ugolev, Inorganic EPR dosimeter for medical radiology. Appl. Radiat. Isot. 52, 1217–1219 (2000).

10. G. M. Hassan and M. Ikeya, Metal ion-organic compound for high sensitive ESR dosimetry. Appl. Radiat. Isot. 52, 1247–1254 (2000).

11. S. K. Olsson, E. Lund and A. Lund, Development of ammonium tartrate as an ESR dosimeter material for clinical purposes. Appl. Radiat. Isot. 52, 1235–1241 (2000).

12. S. Murali, V. Natarajan, R. Venkataramani and M. D. Sastry, ESR dosimetry using inorganic materials: a case study of Li$_2$CO$_3$ and CaSO$_4$:Dy as prospective dosimeters. Appl. Radiat. Isot. 55, 253–258 (2001).

13. D. V. G. Narasimha Rao and W. Gordy, Electron spin resonance of an irradiated single crystal of deuterated DL-tartaric acid. *J. Chem. Phys.* **36**, 1143–1145 (1962).

14. G. C. Moulton and M. P. Cernansky, Electron spin resonance of X-irradiated single crystals of dl-tartaric acid at 77°K. *J. Chem. Phys.* **51**, 2283–2284 (1969).

15. G. C. Moulton and B. Cernansky, ESR studies of deuterated dl-tartaric acid X irradiated at 195°K. *J. Chem. Phys.* **53**, 3022–3025 (1970).

16. M. Gibella, A-S. Crucq, B. Tilquin, P. Stocker, G. Lesgards and J. Raffi, Electron spin resonance studies of some irradiated pharmaceuticals. *Radiat. Phys. Chem.* **58**, 69–76 (2000).